



Ocean Acidification Changes Abiotic Processes but Not Biotic Processes in Coral Reef Sediments

Artur Fink^{1*}, Joost den Haan¹, Arjun Chennu¹, Sven Uthicke² and Dirk de Beer¹

¹ Microsensor Group, Max-Planck Institute for Marine Microbiology, Bremen, Germany, ² Australian Institute of Marine Science, Townsville, QLD, Australia

OPEN ACCESS

Edited by:

Steeve Comeau,
University of Western Australia,
Australia

Reviewed by:

Ulisse Cardini,
University of Vienna, Austria
Anthony William Larkum,
University of Technology Sydney,
Australia

*Correspondence:

Artur Fink
arturfink@mailbox.org

Specialty section:

This article was submitted to
Coral Reef Research,
a section of the journal
Frontiers in Marine Science

Received: 19 December 2016

Accepted: 01 March 2017

Published: 21 March 2017

Citation:

Fink A, den Haan J, Chennu A,
Uthicke S and de Beer D (2017)
Ocean Acidification Changes Abiotic
Processes but Not Biotic Processes in
Coral Reef Sediments.
Front. Mar. Sci. 4:73.
doi: 10.3389/fmars.2017.00073

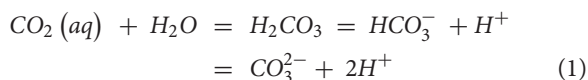
In coral reefs, sediments play a crucial role in element cycling by contributing to primary production and the remineralization of organic matter. We studied how future ocean acidification (OA) will affect biotic and abiotic processes in sediments from two coral reefs of the Great Barrier Reef, Australia. This was investigated in the laboratory under conditions where water-sediment exchange was dominated by molecular diffusion (Magnetic Island) or by porewater advection (Davies Reef). OA conditions ($+\Delta p\text{CO}_2$: 170–900 μatm , $-\Delta\text{pH}$: 0.1–0.4) did not affect photosynthesis, aerobic and anaerobic organic matter remineralization, and growth of microphytobenthos. However, microsensor measurements showed that OA conditions reduced the porewater pH. Under diffusive conditions these changes were limited to the upper sediment layers. In contrast, advective conditions caused a deeper penetration of low pH water into the sediment resulting in an earlier pH buffering by dissolution of calcium carbonate (CaCO_3). This increased the dissolution of Davies Reef sediments turning them from net precipitating ($-0.8 \text{ g CaCO}_3 \text{ m}^{-2} \text{ d}^{-1}$) under ambient to net dissolving ($1 \text{ g CaCO}_3 \text{ m}^{-2} \text{ d}^{-1}$) under OA conditions. Comparisons with *in-situ* studies on other reef sediments show that our dissolution rates are reasonable estimates for field settings. We estimate that enhanced dissolution due to OA will only have a minor effect on net ecosystem calcification of the Davies Reef flat ($<4\%$). However, it could decrease recent sediment accumulation rates in the lagoon by up to 31% (by $0.2\text{--}0.4 \text{ mm year}^{-1}$), reducing valuable reef space. Furthermore, our results indicate that high-magnesium calcite is predominantly dissolving in the studied sediments and a drastic reduction in this mineral can be expected on Davies Reef lagoon in the near future, leaving sediments of an altered mineral composition. This study demonstrates that biotic sediment processes will likely not directly be affected by OA. Ensuing indirect effects of OA-induced sediment dissolution on biotic processes are discussed.

Keywords: coral reef sediments, sediment dissolution, ocean acidification, magnesium calcites, microphytobenthos, hyperspectral imaging, microsenors

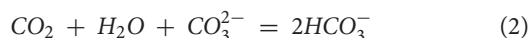
INTRODUCTION

The world's oceans have taken up approximately one third of the anthropogenic carbon dioxide (CO_2) produced since the industrial revolution (Khaliwal et al., 2013). For the end of this century, recent projections suggests an increase in the partial pressure of CO_2 ($p\text{CO}_2$) in the atmosphere from today's 400 μatm to more than 1,300 μatm (Moss et al., 2010).

This leads to ocean acidification (OA), a phenomenon already well measurable (Caldeira and Wickett, 2003). The reaction of CO_2 with seawater enhances the formation of hydrogen ions (H^+ , Zeebe and Wolf-Gladrow, 2001), according to:



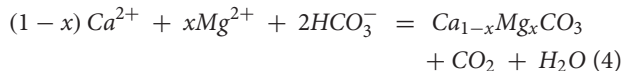
As $\text{pH} = -\log_{10} [\text{H}^+]$, it is expected that the surface ocean pH will decrease by up to 0.4 units by 2100 (Orr et al., 2005). Furthermore, this leads to a concentration decrease of carbonate ions (CO_3^{2-}):



The reduction in CO_3^{2-} concentrations lowers the saturation state (Ω_x) with respect to calcium carbonate (calcite, aragonite) and of Mg-calcite composed of x mol% magnesium:

$$\Omega_x = \frac{[\text{Ca}^{2+}]^{1-x} \times [\text{Mg}^{2+}]^x \times [\text{CO}_3^{2-}]}{K_{sp}^*}, \quad (3)$$

where the square brackets are the concentrations of the ions and K_{sp}^* is the ion concentration product at equilibrium. The precipitation of carbonate minerals (equation 4) is thermodynamically favored when $\Omega > 1$, while $\Omega < 1$ makes dissolution more likely (reversal of equation 4, Zeebe and Wolf-Gladrow, 2001).



The major biogenic carbonate minerals differ in their solubility with aragonite being more soluble calcite, while Mg-calcites with > 8 –12 mol% Mg (high-magnesium calcites, HMC) can be more soluble than aragonite (Plummer and Mackenzie, 1974; Morse et al., 2006).

Of particular concern is the response of coral reefs to OA, since their existence directly depends on reef accretion and thus the net production of carbonate structures over time (Hallock, 1997). This is especially troubling since pCO_2 in coral reefs in the last decades seems to increase 2.5–3.5 times faster than in the open ocean, presumably due to changes in coral reef metabolism (Cyronak et al., 2014; Uthicke et al., 2014). Experimental studies showed that the reductions in Ω will decrease the net ecosystem calcification (NEC) of coral reefs, turning them from a state of net precipitation to a state of net dissolution, with potentially negative consequences for the role and function of reef ecosystems (Andersson and Gledhill, 2013). The expected reductions in NEC are caused by lower rates of calcification (e.g., Leclercq et al., 2002; Langdon et al., 2003; Andersson et al., 2009; Dove et al., 2013) and by increased dissolution rates of existing carbonate structures, including reef sediments (e.g., Andersson et al., 2009; Anthony et al., 2013; Cyronak et al., 2013a; Comeau et al., 2015). Even though much less studied, recent data suggests that the increase in dissolution may be more sensitive to OA than the decrease in calcification (Eyre et al., 2014).

Coral reef sediments play a key role in the recycling of nutrients within the reef (Rasheed et al., 2002; Werner et al., 2006; Rao et al., 2012). The sediments form upon gradual erosion of carbonates mainly from the coral reef framework, calcifying green alga *Halimeda* and benthic foraminifers. Due to their large grain sizes and therefore high permeability, coral reef sediments allow for porewater advection. Compared to the diffusive transport occurring in fine sediments, solute transport via porewater advection is much faster and mainly driven by pressure gradients caused by tides, waves, currents, sediment topography and density gradients (Huettel et al., 2014). This increases the supply of oxygen and enhances the infiltration and trapping of organic matter (OM) from the water column (Huettel et al., 1996), resulting in very high OM remineralization rates. Therefore, sediments act as biocatalytic filters that retain nutrients within coral reefs and therefore contribute to sustain the high biomass and gross primary productivity of coral reefs within oligotrophic environments (Rasheed et al., 2002; Wild et al., 2004; Werner et al., 2006; Rao et al., 2012). Furthermore, coral reef sediments are also places of high photosynthesis rates, which can contribute significantly to the ecosystem's primary production (Werner et al., 2008; Schoon et al., 2010; Rao et al., 2012; van Hoytema et al., 2016). Photosynthesis in sediments is mainly carried out by microphytobenthos (MPB), which is an important food source for higher trophic levels (e.g., fish, sea cucumbers).

The carbonate chemistry of reef sediments and therefore their sensitivity toward OA is largely controlled by the interplay between the carbonate chemistry of the overlying water column, benthic photosynthesis and respiration, and transport processes. Increased pCO_2 , as from OA, reduces the water column Ω , which acts as the starting point for any changes in carbonate chemistry within the sediments (Andersson and Gledhill, 2013). The consumption of CO_2 by photosynthesis in illuminated surface sediments can increase porewater pH and Ω , thereby causing the abiotic precipitation of carbonates (Schoon et al., 2010; Rao et al., 2012). In turn, CO_2 release from OM remineralization in the dark and in deeper sediments reduces Ω , leading to carbonate dissolution. It has been suggested that the increased dissolution under OA is caused by more OM remineralization occurring when $\Omega < 1$ with respect to the most soluble carbonate mineral has been reached, a condition referred to as Carbonate Critical Threshold (CCT; Andersson, 2015). On coral reefs, high-magnesium calcites mainly formed by red coralline algae, benthic foraminifers, bryozoans and echinoderms, have been proposed to dissolve first under OA (Morse et al., 2006; Andersson et al., 2007; Haese et al., 2014). Furthermore, the degree to which the water column conditions will translate into the sediment porewater depends on transport processes. For example, Cyronak et al. (2013a) showed that OA-induced dissolution of coral reef sediments was doubled under conditions of porewater advection as compared to diffusion. The authors suggested that this could be due to a deeper penetration of low pH water into the sediment under advective conditions. However, to date there are no measurements of porewater carbonate chemistry within reef sediments under OA conditions and under different transport processes.

This study presents the results of two independent experiments that aimed to document the effect of transport on the porewater pH within carbonate reef sediments under OA conditions. For this, we exposed carbonate sediments from the Great Barrier Reef to conditions where sediment-water exchange was dominated by either diffusion or advection. Sediments from Magnetic Island (an inshore fringing reef) were studied under diffusive conditions, while sediments from Davies Reef (a classical mid-shelf platform reef) were investigated under advective conditions. The effects of OA on porewater pH were determined using microsensors.

We hypothesized that high CO_2 could stimulate microphytobenthic primary production, changing the rate of sediment processes and porewater pH. Therefore, we also monitored the activity and growth of microphytobenthos, and determined fluxes of dissolved organic carbon, nutrients, total alkalinity as a measure for dissolution and organic matter mineralization via oxygen respiration and sulfate reduction.

MATERIALS AND METHODS

Sampling

Sediment from the central section of the Great Barrier Reef (Australia) were collected from a fringing near-shore reef off Magnetic Island (Geoffrey Bay) in May 2014 and from the reef flat of Davies Reef, a mid-shelf coral reef in May 2015. Sediments were transported to the facilities of the National Sea Simulator (SeaSim) at the Australian Institute of Marine Science (Townsville, Queensland, Australia) on the day of collection. Prior to the start of experiments, sediment were maintained in flow-through aquaria receiving 2 L min^{-1} filtered seawater of ambient pCO_2 under low light conditions ($\sim 20 \mu\text{mol photons m}^{-2} \text{ s}^{-1}$). The sediments were sieved ($< 2 \text{ mm}$) to remove most macrofauna, homogenized and, inundated with filtered water ($< 0.2 \mu\text{m}$), added into chambers and flumes of the respective experiments.

Experimental Setup

Magnetic Island sediments were studied under diffusive conditions for 14 days. Sediments were placed into flumes with a working section ($20 \times 25 \text{ cm}$) to a height of 5 cm, covered by a 5 cm high water column. Each flume received seawater of either target pCO_2 of ~ 400 ("Control"), ~ 600 ("Medium"), and $\sim 800 \mu\text{atm}$ ("High") at an inflow rate of 1.2 L min^{-1} (3 flumes per pCO_2 treatment). The unidirectional flow had a velocity of $\sim 1 \text{ cm s}^{-1}$ and was passed through a diffuser to create laminar flow above the sediment. A light:dark cycle of 12:12 h with a ramp time of 1 h was established by white and blue LED modules (Sol White, Aqua Illumination, USA). The photosynthetically active radiation (PAR) at the sediment surface was $\sim 350 \mu\text{mol photons m}^{-2} \text{ s}^{-1}$. Davies Reef sediments were studied under advective conditions for 9 days. A 10 cm thick sediment layer was incubated under a 16 cm high water column within acrylic cylindrical chambers (diameter: 19 cm) that were sealed with a light-permeable lid. Each chamber received seawater at an inflow rate of 0.15 L min^{-1} with three chambers each under a

pCO_2 treatment of ~ 400 ("Control") and $\sim 1300 \mu\text{atm}$ ("High"). The water column was stirred by a transparent rotating disc (15 cm diameter, 1 cm thick) mounted 10 cm above the sediment surface. The disk rotated with 40 rpm, which was shown to create pressure gradients of $\sim 2.5 \text{ Pa}$ between the center and the edges of the chamber (Janssen et al., 2005). This is similar to the pressure gradients occurring at current velocities between 10 and 20 cm s^{-1} (Huettel et al., 1996), which are frequently encountered on Davies Reef flat (Pickard, 1986). The light conditions were the same as for the diffusive experiment.

Carbon Chemistry Manipulation and Monitoring

The seawater used for experiments was collected 500 m offshore from SeaSim, filtered and brought to the experimental temperature (Table 1). The respective pCO_2 levels were achieved using pure CO_2 as described by Ow (2016). pH was measured daily using a multi-parameter meter (HQ40d, Hach) with a glass electrode (IntelliCALTM pH, PHC201) calibrated with pH_{NBS} buffers. The pH measurements were recalculated on the total scale (pH_{T}) by offset-correction using photometric pH measurements with Tris-buffered saline or m-Cresol (Dickson et al., 2007). On 3 days 250 mL of the overlying water was sampled and poisoned by addition of 125 μL of a saturated mercury chloride solution for analysis of total alkalinity (TA) by acid titration (Vindta 3C, Marianda, Germany).

Carbon Chemistry Calculations

The carbonate chemistry in the water column (Table 1) and porewater was calculated using the software package "seacarb" for R (Lavigne et al., 2011; R Core Team, 2015). Using the "carb" function we calculated pCO_2 , dissolved inorganic carbon (DIC), and the saturation states of calcite (Ω_{calc}) and aragonite (Ω_{arag}) from TA, pH_{T} , temperature and salinity. To calculate the saturation states of the high-magnesium calcite (Ω_{HMC}) we utilized the function "Om" that computes Ω_{HMC} using the Mg-content vs. stability curve for minimally prepared biogenic Mg-calcites of Plummer and Mackenzie (1974).

To estimate porewater Ω , we used the measured porewater pH and a wide range of TA concentrations ranging between water column concentrations of 2,320–2,360 $\mu\text{mol kg}^{-1}$ and 4,000 $\mu\text{mol kg}^{-1}$.

Sediment Characteristics

Porosity of the upper 0–1 cm was determined as the weight loss of a known volume of sediment after freeze-drying. Freeze-dried samples were used to determine total carbon (TC), total nitrogen (TN), and (after decalcification) total organic carbon (TOC) using an elemental analyzer (Euro EA 3000, EuroVector). Total inorganic carbon (TIC) was calculated as the difference between TC and TOC.

Grain size distributions obtained by dry-sieving (60°C , until constant weight) using a calibrated sieve stack were used to graphically determine the median grain size with the program GSSTAT; Poppe et al., 2004). For sediments incubated under advective conditions, the permeability of the upper 4 cm was

TABLE 1 | Carbonate chemistry parameters over the experimental period of the diffusive and advective experiments.

pCO ₂ treatment	pH _T	TA (μmol kg ⁻¹)	pCO ₂ (μatm)	DIC (μmol kg ⁻¹)	Ω _{calc}	Ω _{arag}	Ω _{HMC}	Temperature (°C)	Salinity
DIFFUSIVE EXPERIMENT (MAGNETIC ISLAND)									
Control	8.00 ± 0.00	2317 ± 1	457 ± 4	2031 ± 2	5.01 ± 0.03	3.32 ± 0.02	1.12 ± 0.01	27.3 ± 0.0	34 ± 0
Medium	7.88 ± 0.00	2318 ± 1	628 ± 0	2095 ± 1	4.04 ± 0.00	2.68 ± 0.00	0.91 ± 0.00	27.2 ± 0.0	34 ± 0
High	7.76 ± 0.00	2317 ± 0	835 ± 0	2144 ± 0	3.28 ± 0.00	2.17 ± 0.00	0.74 ± 0.00	27.1 ± 0.0	34 ± 0
ADVECTIVE EXPERIMENT (DAVIES REEF)									
Control	8.01 ± 0.00	2360 ± 0	441 ± 4	2075 ± 4	4.99 ± 0.03	3.29 ± 0.02	1.20 ± 0.01	25.5 ± 0.0	34 ± 0
High	7.61 ± 0.00	2363 ± 0	1338 ± 18	2270 ± 4	2.22 ± 0.03	1.46 ± 0.02	0.54 ± 0.05	25.5 ± 0.1	34 ± 0

Partial pressure of carbon dioxide (pCO₂), dissolved inorganic carbon (DIC), and the saturation states of calcite (Ω_{calc}), aragonite (Ω_{arag}) and high-magnesium calcite (Ω_{HMC}) were calculated from pH_T, total alkalinity (TA), temperature and salinity. Data are mean ± SE. *n* = 7 for pH_T, temperature and salinity. *n* = 3 for the other parameters.

determined with the falling-head method (Klute and Dirksen, 1986).

X-Ray Diffraction

The mineralogical composition of the sediments was measured by X-ray diffraction. Dried bulk samples were pulverized (<20 μm particle size) and prepared with the Philips backloading system. The X-ray diffraction was measured on a Philips X'Pert Pro multipurpose diffractometer. Identification of the minerals was performed using the Philips software X'Pert HighScore™. Semi-quantification of each mineral was based on Relative Intensity Ratio values calculated after Chung (1974). Mg-content of Mg-rich calcites was derived from reference minerals provided by the International Centre for Diffraction Data database.

Porewater Microsensor Profiles

The pH and oxygen microsensors were built, calibrated and used as described in de Beer et al. (1997) and Revsbech (1989), respectively. The tip size of the pH microsensors was 150 μm and a response time (*t*₉₀) of <10 s. The oxygen microsensors had a tip size of 150 μm and a response time (*t*₉₀) of <5 s. Details on the microsensor setup are described in Polerecky et al. (2007). In the diffusive experiment, parallel porewater profiles of O₂ and pH (step size: 400 μm) were obtained in the dark and light beginning after 4 h at the respective condition. Due to the measurement duration of each profile (10–15 min) and in order to increase replication, the data of 2–4 days were pooled. In the advective experiment, porewater pH profiles in the dark were obtained using a vertical steps size of 500 μm close to the wall (position A), between center and wall (position B) and in the center (position C) of each chamber on day 9. For this, the flow-through system was interrupted, the chamber lids and stirring discs were removed and the overlying water was decreased to a height of 10 cm. During the measurements, the water was gently mixed by a submersible pump at a velocity 1 cm s⁻¹.

Microphytobenthos Growth

Hyperspectral imaging was used to non-destructively estimate the abundance of MPB biomass from the chlorophyll content at the sediment surface over the duration of the advective experiment, following the methodologies described by Polerecky et al. (2009) and Chennu et al. (2013, 2015). The hyperspectral imager (Pika II; Resonon, United States) was mounted on a

moveable rig and, during the scan of the chambers, captured back-scattered light off the sediment in 480 spectral bands (~2 nm resolution) over the range of 430–900 nm. During scanning, the sediments were illuminated by broadband light delivered by a light chain (GS-TZ-10, Taizhoe Tianze Lamp Industries Co Ltd., China) radially arranged around the chamber walls. The sediment's chlorophyll content was estimated from the logarithmic difference of the reflectance at the wavelengths of *in-vivo* chlorophyll absorption maximum (666 nm) and edge (703 nm). This calculation was performed at each pixel, and the values averaged over the imaged area of the sediment scanned. To calibrate the hyperspectral imaging signal for actual chlorophyll *a* content, three sediment cores (diameter: 2.8 cm) were inserted into each of the six chambers at the end of the experiment. From each core, the sediment surface was imaged and subsequently the top 5 mm of the sediment was sliced for chlorophyll *a* determination, and regression against the spectral index for chlorophyll. The MPB biomass was also estimated at the end of the diffusive experiment. For this, the upper 3 mm of the sediments on three randomly selected positions in each flume were collected for photopigment analysis using core liners (diameter: 1 cm). Photopigment samples from both experiments were immediately frozen (−80°C), photopigments were extracted as described by Al-Najjar et al. (2012) and measured using the HPLC method after Wright et al. (1991).

Net Photosynthesis and Oxygen Consumption

Net photosynthesis in the light and oxygen consumption in the dark was measured in both experiments. In the diffusive experiment, oxygen fluxes (JO₂) were calculated from the oxygen profiles according to Fick's first law of diffusion

$$JO_2 = DO_2 \frac{d[O_2]}{dz},$$

where DO₂ is the diffusion coefficient of oxygen, [O₂] is the oxygen concentration and *z* is the depth. The JO₂ was calculated for the upper 0–1.5 mm of the sediment taking into account porosity (φ) and the diffusion coefficient was corrected for tortuosity (θ, D'O₂ = DO₂/θ²) adjusted for sands (θ² = φ^{1-m}, *m* = 2; Boudreau, 1997). Oxygen flux measurements in the advective experiment were performed on day 8. The

water flow-through was interrupted and water column oxygen concentrations were measured before and after an incubation of 2–3 h. Oxygen fluxes were calculated as the concentration difference between the start and the end of an incubation taking into account the volume of the overlying water, the sediment surface area and the incubation time. To investigate the short-term response of low pH on oxygen consumption in sediments used for the advective experiment, we measured volumetric oxygen consumption rates by the percolation method described in de Beer et al. (2005). Homogenized sediment was filled into a core liner (diameter: 5 cm), which was closed from below with a rubber stopper containing a valve that allowed the percolation of water. The sediment was constantly covered by a 5 cm high column of air-saturated water with a pH_T of either 8.03 or 7.54, which was continuously percolated downward through the sediment at a rate of 30 mL min^{-1} . Using oxygen and pH microsenors, the values at 1 cm below the sediment surface were monitored. Once the values were constant, the percolation was stopped and the dynamics of oxygen and pH were monitored. The same procedure was then repeated with pH_T 7.54 water ($n = 1$ for each pH condition).

Sulfate Reduction Rates

Sulfate reduction rates (SRR) were measured in sediments of the diffusive experiment using the whole core injection method according to Jørgensen (1978). On the last experimental day, one sediment core (26 mm diameter) was retrieved from each flume. Using a syringe with a hypodermic needle, $50 \mu\text{L } ^{35}\text{SO}_4^{2-}$ ($\sim 1000 \text{ kBq}$) was vertically injected into each core, distributing an equal amount of tracer into each depth layer. After incubation for 6–6.5 h in the dark in a water bath (25.5°C), sediment cores were frozen (-20°C), sliced into depth intervals of 0–0.5, 0.5–1.5, 1.5–3, 3–5 cm and fixed in 10 mL of 20% (w/v) zinc acetate. Volumetric SRR were determined by the single-step chromium distillation technique after Kallmeyer et al. (2004) as modified by Røy et al. (2014). Porewater sulfate concentrations were determined by non-suppressed anion exchange chromatography (Metrohm 761 Compact IC, Herisau, Switzerland). Areal SRR were calculated by integrating the volumetric SRR over the measured sediment column.

Solute Fluxes

Fluxes of dissolved organic carbon (DOC), nutrients and total alkalinity were measured in the advective experiment from water samples used for oxygen flux measurements. Samples for DOC were fixed using $250 \mu\text{L HCl}$ and stored at 4°C until analysis using a TOC analyzer (Shimadzu TOC-5000A, Japan). Nutrient samples (Si , PO_4^{3-} , $\text{NO}_2^- + \text{NO}_3^-$, NO_2^-) were filtered through $0.2 \mu\text{m}$ cellulose-acetate filters, frozen (-20°C) and analyzed using standard methods (Ryle et al., 1981). Total alkalinity (TA) samples of 50 mL were poisoned with $100 \mu\text{L}$ of a saturated HgCl_2 solution and kept with no headspace until measurement by automatic gran titration using a Metrohm 855 titrosampler (Metrohm, Switzerland) as described by Vogel et al. (2016). The TA anomaly technique (Chisholm and Gattuso, 1991) was used to calculate net CaCO_3 fluxes, assuming that the ratio in fluxes between TA and CO_3^{2-} is 2:1.

Statistical Analysis

All statistical tests were performed using the statistical software R (R Core Team, 2015). To test for differences between means of pCO_2 treatments we used the analysis of variance (ANOVA) for the diffusive experiment (three treatment levels) and t -test for the advective experiment (two treatment levels) at a significance level of $p < 0.05$. All data was first tested for normal distribution and homogeneity of variances.

RESULTS

Sediment Characteristics

Within each experiment the sediment characteristics were similar in all pCO_2 treatments (Supplementary Table 1). Sediments from both Magnetic Island and Davies Reefs were carbonate sands (TIC content: 11.2–11.6% dry weight) with a similar median grain size ($\sim 0.49 \text{ mm}$) and the carbonate minerals were dominated by aragonite (83–85%), followed by 10–11% HMC (13%-Mg-calcite). Sediments used for the advective experiment were highly permeable ($1.3\text{--}1.4 \times 10^{-11} \text{ m}^2$).

Microphytobenthic Growth

The pCO_2 treatments had no differential effects on the growth of MPB in both the diffusion- (Supplementary Table 2) and advective experiment (Figure 1). The horizontal distribution of MPB biomass in sediments of the advective experiment was heterogeneous, with a local maximum in the center of all chambers (Figure 1A). The spectral signal vs. the actual chlorophyll a concentration showed a linear relationship with $R^2 = 0.62$ (data not shown). In both experiments, the MPB was dominated by diatoms as indicated by high concentrations of fucoxanthin (a marker pigment for diatoms; Supplementary Table 2).

Net Photosynthesis and Oxygen Consumption

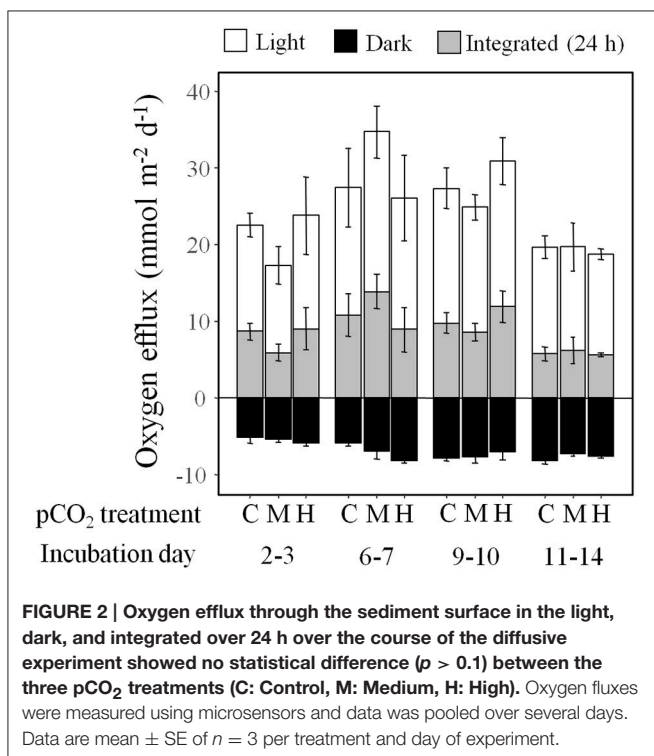
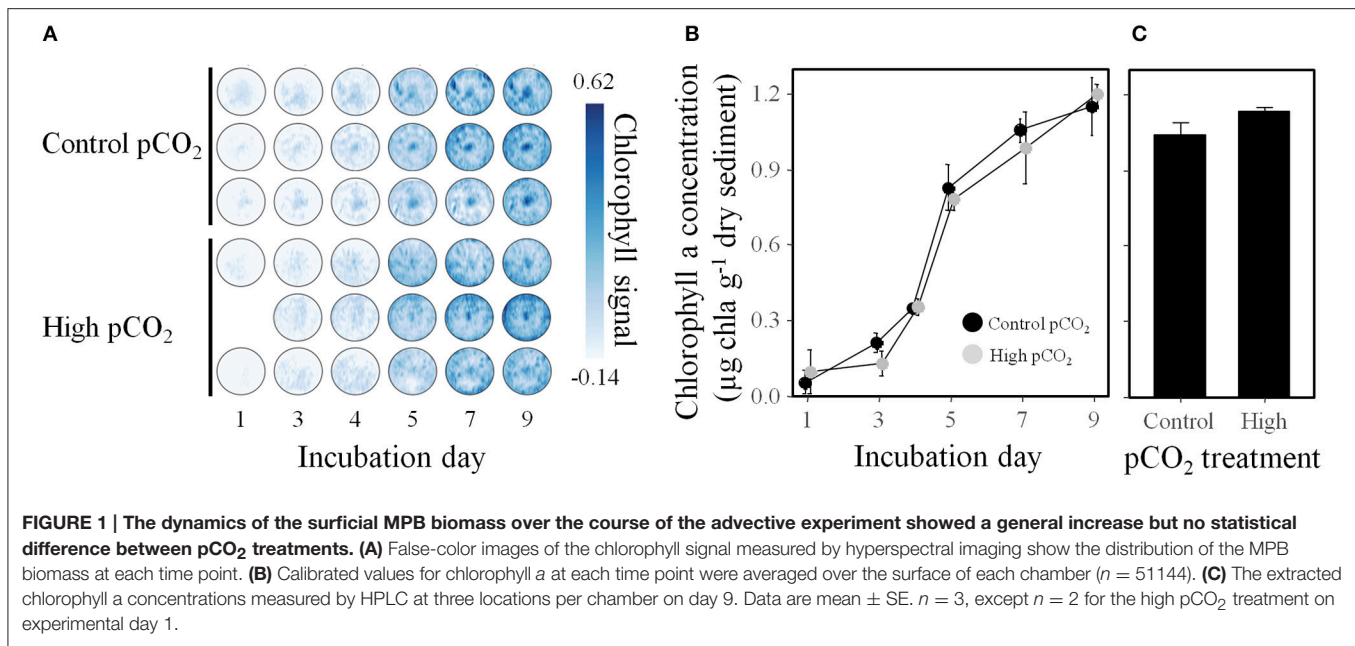
Net photosynthesis in the light and oxygen consumption in the dark were not influenced by the pCO_2 level in the diffusive (Figure 2) and advective experiment (Figure 3). Over 24 h the sediments were net autotrophic, releasing 3–18 and 37–47 $\text{mmol O}_2 \text{ m}^{-2} \text{ d}^{-1}$, respectively. Volumetric oxygen consumption rates in sediments used for the advective experiment were not affected by the pCO_2 treatment on the short-term ($4.5 \mu\text{mol O}_2 \text{ L}^{-1} \text{ min}^{-1}$, Figure 4). This was measured at a depth of 1 cm using the percolation method. During the period when oxygen was still present, the porewater pH decreased to 7.95 when the initial porewater pH was 8.03 (Figure 4A), and remained stable when the initial porewater pH was 7.54 (Figure 4B).

Sulfate Reduction Rates

Average areal sulfate reduction rates in the diffusive experiment were not affected by the pCO_2 treatment (Table 2) and contributed 4–12% to the total carbon mineralization.

Solute Fluxes

Under advective conditions, the net precipitation of CaCO_3 in the light at high pCO_2 was 5.8 times lower than under



control pCO₂ (Figure 3B). In the dark, the CaCO₃ dissolution was increased 2.7-fold under high pCO₂. On a daily basis the sediments were net precipitating CaCO₃ under control pCO₂, while they were net dissolving under high pCO₂. The nutrient and DOC fluxes were not influenced by the pCO₂ treatment nor light conditions (Supplementary Table 3).

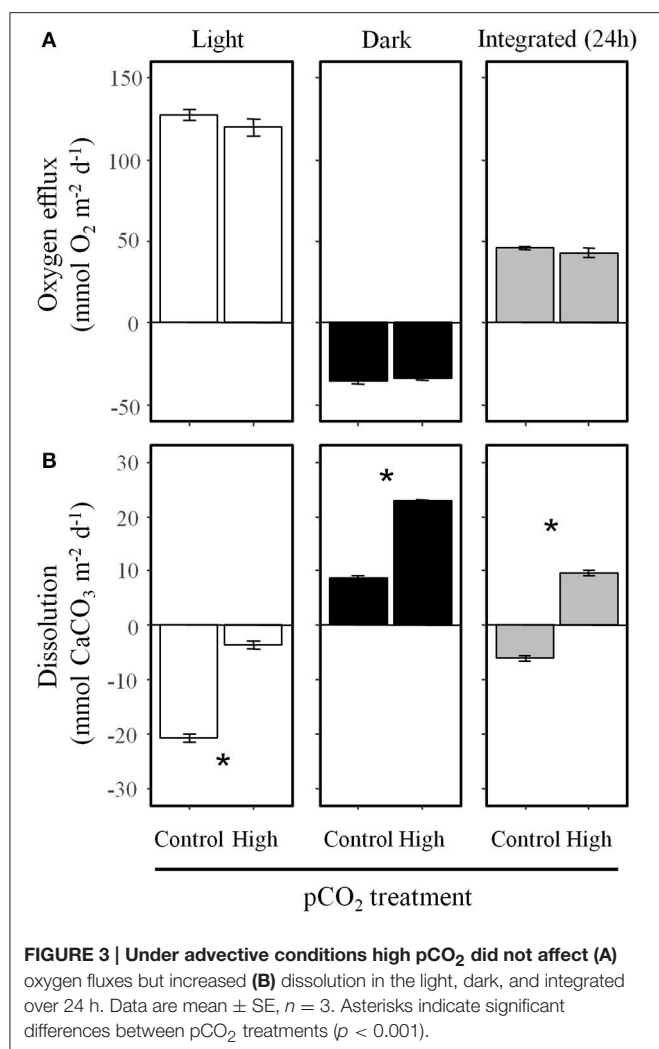
Porewater Microprofiles

Under diffusive conditions, the oxygen profiles in the light and in the dark were similar between all pCO₂ treatments (Figure 5A), showing that the pCO₂ treatment had no effects on oxygen production and consumption. When illuminated by light, the porewater pH in the upper 5 mm was influenced by the water column pH (Figure 5B). Namely, the peak in porewater pH at ~ 2 mm caused by photosynthetic activity of the MPB decreased with decreasing water column pH. In the dark, the influence of reduced water column pH was less pronounced, but resulted in a lower porewater pH close to the sediment surface (4–6 mm). At 1 cm depth the porewater pH approached 7.4–7.6 with increasing depth both in the dark and the light. In the advective experiment, the patterns in porewater pH followed the porewater flow path in the stirred chambers (Figure 6). The water column pH had the largest influence on the porewater pH in the inflow region at the edge of the chamber (position A) and in the upper 3–5 mm at the other positions. The porewater pH decreased along the porewater flow path from the edge to the center of the chamber (position C) with both pCO₂ treatments reaching a final pH of ~ 7.5 at depths > 5 mm. The high pCO₂ treatment showed this pH already at position B, while the pH was 0.1–0.2 units higher in the control pCO₂ treatment.

DISCUSSION

Elevated pCO₂ Does Not Affect Biotic Processes

Our study demonstrates in two independent experiments that medium-term exposure to elevated pCO₂ does not significantly influence biotic processes associated with photosynthesis and OM remineralization in coral reef sediments. A lack of pH



effects could be explained by the pH conditions typically experienced by sediment microorganisms. Close to the sediment surface, microorganisms carrying out photosynthesis and aerobic respiration may be adapted to wide pH ranges due to diel pH variations up to 1 unit caused by their own activity (Werner et al., 2008; Schoon et al., 2010; Rao et al., 2012). In contrast, the similar sulfate reduction rates at all pCO₂ levels in the diffusive experiment can be explained by the buffered porewater pH in deeper sediment layers, where a major part of sulfate reduction occurs.

We expected a stimulation of photosynthesis and MPB growth by elevated pCO₂, reducing a possible CO₂ limitation that can occur when high photosynthetic activity shifts the carbonate system away from CO₂ (Cook and Røy, 2006). The absence of any CO₂ limitation could be due to the following reasons. First, the MPB community in our experiments was dominated by diatoms, which are known to possess very efficient carbon concentrating mechanisms that convert HCO₃⁻ to CO₂ (Reinfelder, 2011). Second, porewater advection can relieve MPB from CO₂ limitation by a rapid resupply of free CO₂ (Cook and Røy, 2006). Third, MPB may have been limited by inorganic

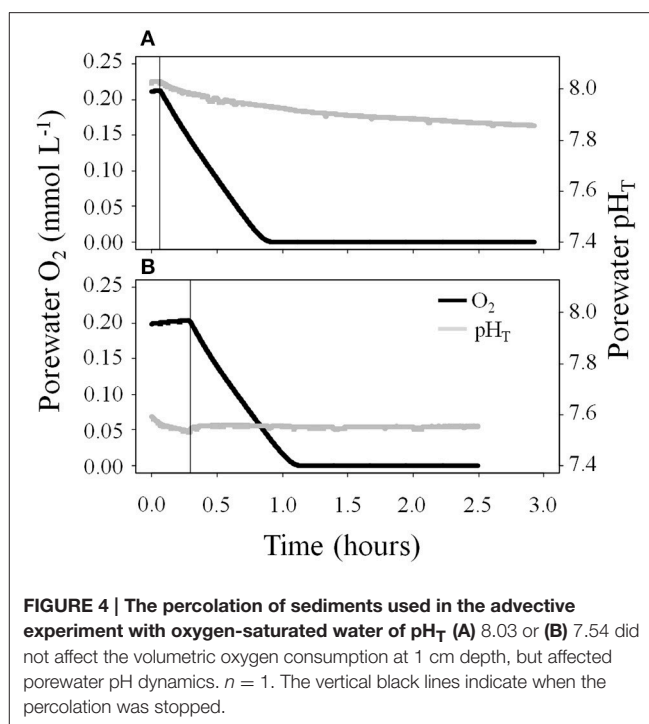


TABLE 2 | Volumetric and areal sulfate reduction rates (SRR) in sediments of the diffusive experiment were not influenced by the pCO₂ treatment (*p* > 0.05).

SRR	Depth (cm)	pCO ₂ treatment		
		Control	Medium	High
Volumetric (nmol cm ⁻³ d ⁻¹)	0.0–0.5	1.5 ± 0.9	6.5 ± 1.5	15.8 ± 6.0
	0.5–1.5	19.7 ± 4.9	23.5 ± 7.0	22.2 ± 5.0
	1.5–3.0	25.1 ± 3.2	40.7 ± 16.0	28.1 ± 6.8
	3.0–5.0	20.0 ± 7.0	26.7 ± 3.5	13.3 ± 3.2
	0.0–5.0	0.98 ± 0.23	1.41 ± 0.26	0.99 ± 0.07
Areal (mmol m ⁻² d ⁻¹)				
0.0–5.0				

Data are mean ± SE, *n* = 3.

nutrients rather than CO₂ (Uthicke and Klumpp, 1998). This is supported by the observation of the highest MPB biomass in the center of the advective chambers, where the longest flow path of porewater emerge at the surface, thus supplying the highest nutrient load (Huettel and Gust, 1992). Similar to our study neither photosynthesis nor OM remineralization were affected by elevated pCO₂ in coral reef sediments in Heron Island (GBR, Australia, Anthony et al., 2013; Cyronak et al., 2013a; Cyronak and Eyre, 2016; Trnovsky et al., 2016) and Moorea (French Polynesia, Comeau et al., 2014, 2015). However, in reef sediments from Sesoko Island (Okianwa, Japan) high pCO₂ stimulated photosynthesis and bacterial growth, while oxygen consumption was reduced (Sultana et al., 2016). Thus, biotic responses toward OA in reef sediments may differ between coral reefs suggesting the need for further study.

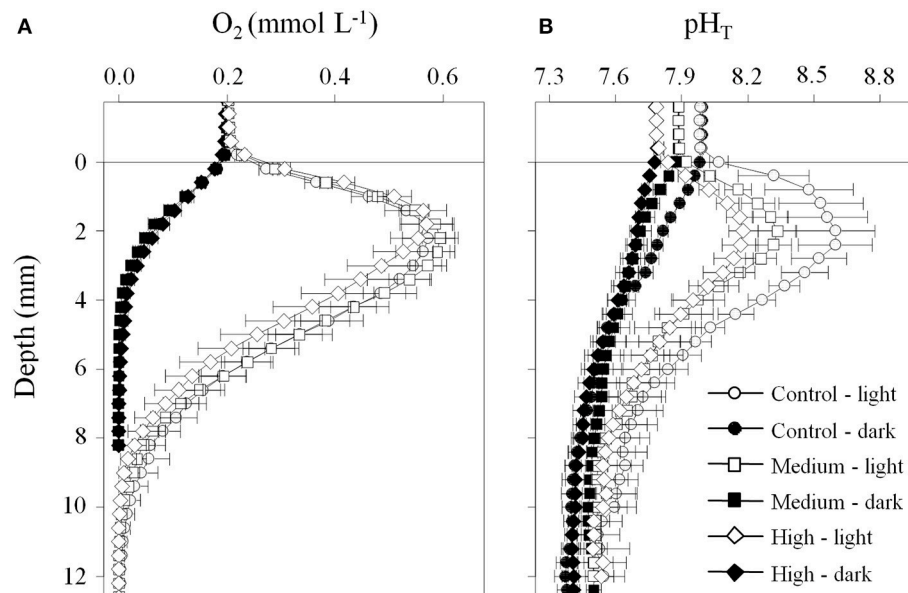


FIGURE 5 | Porewater microsensor profiles of (A) oxygen and (B) pH_T measured in sediments incubated under diffusive conditions show that the porewater pH is affected by respiration and photosynthesis, and the pH of the overlying water. Profiles were measured on days 9 and 10 of the experiment. Data are mean \pm SE, $n = 3$. The horizontal line at 0 mm depth indicates the sediment surface.

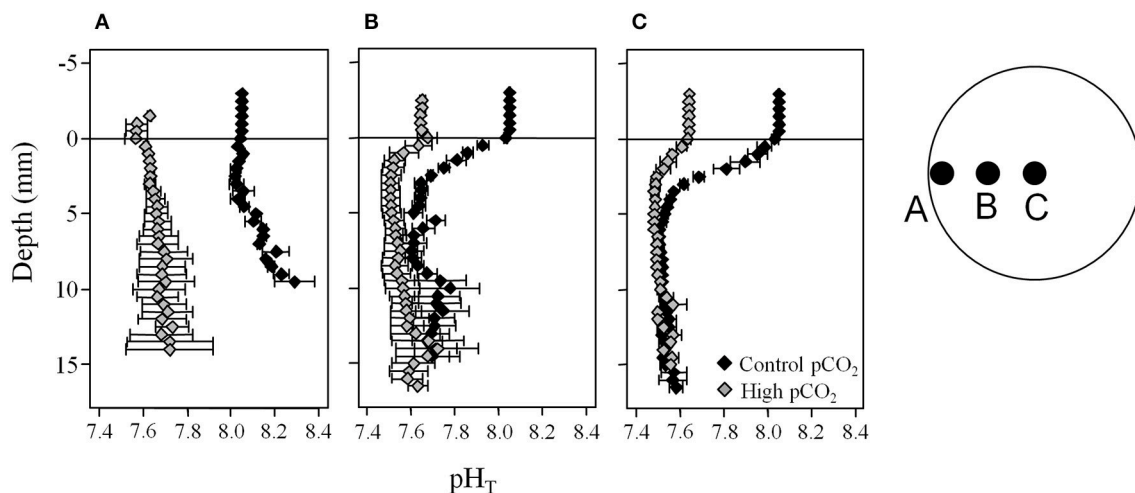


FIGURE 6 | Porewater pH_T profiles in sediments of the advective experiment show that along the porewater flow path from the edge to the center of the chamber the porewater pH is buffered earlier at high pCO_2 compared to control pCO_2 . Measurements were conducted at (A) one centimeter away from the wall, (B) halfway between the center and the wall, and (C) the center of the chamber in the dark (see insert showing the top view onto the sediment surface). At each depth data are shown as mean \pm SE, $n = 3$. The horizontal line at 0 mm depth indicates the sediment surface.

Elevated pCO_2 Increases $CaCO_3$ Dissolution

OA conditions drastically increased $CaCO_3$ dissolution in the advective experiment on Davies Reef flat sediments by changing the carbonate chemistry in the porewater. High pCO_2 turned the sediments from net precipitating ($-6.0 \text{ mmol } CaCO_3 \text{ m}^{-2} \text{ d}^{-1}$) to net dissolving ($9.7 \text{ mmol } CaCO_3 \text{ m}^{-2} \text{ d}^{-1}$) on a daily basis. Even though we made no measurements of $CaCO_3$ dissolution

in the diffusive experiment, the lower porewater pH at elevated pCO_2 in the light and in the dark indicates a lower porewater Ω . This likely resulted in lower photosynthetic $CaCO_3$ precipitation in the light and increased dissolution in the dark that has also been described for other reef sediments under diffusive conditions (Cyronak et al., 2013a).

Although the two experiments are not directly comparable, generally higher dissolution rates can be expected under

advective than diffusive conditions under similar $p\text{CO}_2$ conditions due to a deeper penetration of low Ω water into the sediments under advective conditions (Cyronak et al., 2013a). Indeed, in the advective experiment the water column pH affected deeper sediment layers, particularly at the inflow region of the stirred chambers. In contrast, in the diffusive experiment differences in porewater pH were limited to the upper sediment layers. Irrespective of the $p\text{CO}_2$ level and solute transport regime, an increase in sediment dissolution has been found by all studies under elevated $p\text{CO}_2$ (Anthony et al., 2013; Cyronak et al., 2013a; Comeau et al., 2014, 2015; Cyronak and Eyre, 2016; Trnovsky et al., 2016), suggesting that this OA response is common of coral reef sediments.

It has been suggested that sediment dissolution occurs faster under high $p\text{CO}_2$ because less metabolic CO_2 is required to reach the CCT, so that more metabolic CO_2 can drive dissolution (Andersson, 2015). This is supported by the temporal and spatial patterns in porewater pH in sediments studied under advective conditions. In the percolation experiment, an initial pH of 8.0 was reduced by metabolic CO_2 from aerobic respiration, suggesting that the CCT was not reached. In contrast, the CCT was likely reached at an initial porewater pH of 7.5 so that metabolic CO_2 addition resulted in dissolution that buffered the pH. This can also explain the patterns in porewater pH in the stirred chambers. Along the flow path from the chamber edge toward the center, the porewater accumulates metabolic CO_2 . At high $p\text{CO}_2$ the CCT was reached already in the middle of the porewater flow path, because the pH of 7.5–7.6 did not decrease further along the path. Even though such low pH also occurred at control $p\text{CO}_2$, the pH gradually decreased along the flow path, indicating that the CCT was reached later and only close to the outflow. As the CCT is reached earlier at high $p\text{CO}_2$, more metabolic CO_2 is available to drive dissolution beyond the CCT. At similar CO_2 production rates this will result in increased sediment dissolution under high $p\text{CO}_2$, which we observed.

Our calculations of porewater Ω indicate that high-magnesium calcites (HMC) are the predominantly dissolving minerals. The porewater pH in sediments studied under both diffusion- and advective-dominated conditions never decreased below 7.4–7.6, demonstrating that the pH is buffered by the dissolution of the carbonate sediments. At decreased pH they start dissolving, thus stabilizing the pH. The studied sediments were both enriched in HMC (13%-Mg-calcite), which was the most soluble carbonate mineral present. In all elevated $p\text{CO}_2$ treatments the water column was undersaturated with respect to HMC, but not to aragonite. We calculated the porewater Ω using the minimum porewater pH_T of 7.4–7.6 and a wide range of TA concentrations ranging between water column concentrations (2,320–2,360 $\mu\text{mol kg}^{-1}$) and 4,000 $\mu\text{mol kg}^{-1}$ that are rarely exceeded in coral reef sediments (e.g., Andersson, 2015; Yamamoto et al., 2015; Drupp et al., 2016). Indeed, this resulted in undersaturating conditions with respect to HMC ($\Omega_{\text{HMC}} = 0.33\text{--}0.89$), but not to aragonite ($\Omega_{\text{arag}} \geq 1$). This suggests that HMC is the dissolving phase in both studied sediments rather than the much more abundant aragonite. While the preferential dissolution of HMC is in line with findings in natural reef sediments (Andersson et al., 2007; Drupp et al.,

2016), conditions of $\Omega_{\text{arag}} < 1$ cannot be ruled out entirely as they still could occur in microenvironments (e.g., in hot spots of particulate organic matter, in grain crevices).

Ecological Consequences of Sediment Dissolution

Comparing the oxygen fluxes and dissolution rates in the Davis Reef sediments with results from *in-situ* studies on Heron Island shows that our rates are realistic for reef settings. Oxygen fluxes measured in our study are in the range of *in-situ* measurements on the Heron Island reef flat during daytime (-167 to -16 $\text{mmol O}_2 \text{ m}^{-2} \text{ d}^{-1}$), night (14 to 114 $\text{mmol O}_2 \text{ m}^{-2} \text{ d}^{-1}$), and on a daily basis (-26 to 25 $\text{mmol O}_2 \text{ m}^{-2} \text{ d}^{-1}$, Rao et al., 2012; Cyronak et al., 2013b; Cyronak and Eyre, 2016). Also our CaCO_3 dissolution rates in the control $p\text{CO}_2$ treatment are similar to *in-situ* estimates of dissolution during daytime (-86 to -2 $\text{mmol CaCO}_3 \text{ m}^{-2} \text{ d}^{-1}$), night (4 to 57 $\text{mmol CaCO}_3 \text{ m}^{-2} \text{ d}^{-1}$), and on a daily basis (-15 to 16 $\text{mmol CaCO}_3 \text{ m}^{-2} \text{ d}^{-1}$, Rao et al., 2012; Cyronak et al., 2013a,b; Cyronak and Eyre, 2016). Furthermore, the increase in daily dissolution by 16 $\text{mmol CaCO}_3 \text{ m}^{-2} \text{ d}^{-1}$ is only slightly higher than the $7\text{--}11$ $\text{mmol CaCO}_3 \text{ m}^{-2} \text{ d}^{-1}$ found in *in-situ* manipulation experiments that used the same stirring rate, but applied lower $p\text{CO}_2$ ($800\text{--}950$ μatm , Cyronak et al., 2013a; Cyronak and Eyre, 2016). This indicates that our rate estimates are reasonable and can be used to assess the ecological consequences of increased dissolution under high $p\text{CO}_2$ for Davis Reef.

The increase in sediment dissolution caused by OA will have only a small effect on NEC on Davies Reef flat. The current average NEC of the reef flat of 120 $\text{mmol CaCO}_3 \text{ m}^{-2} \text{ d}^{-1}$ (Albright et al., 2013) are 7.5 times higher than the increase in dissolution rates under high $p\text{CO}_2$. Since sediments cover less than 30% of the flat area (Klumpp and McKinnon, 1989; Albright et al., 2013), the increase of dissolution rates will decrease NEC on Davies Reef flat by $<4\%$. However, sediment dissolution effects on NEC will be higher on reefs or reef areas with lower NEC and higher sediment cover (Comeau et al., 2015; Cyronak and Eyre, 2016). Therefore, future declines in calcification (e.g., Andersson et al., 2009; Dove et al., 2013) and increased bioerosion rates (e.g., Wisshak et al., 2012; Reyes-Nivia et al., 2013) could significantly increase the relative importance sediment dissolution for NEC.

Sediment dissolution rates will likely be higher in the Davis Reef lagoon, because it is deeper ($5\text{--}27$ m, average 16 m, Pickard, 1986) than the reef flat and there is less light for photosynthesis. Sediment dissolution increases when the ratio between daily gross photosynthesis and respiration (P/R) decreases (Rao et al., 2012; Cyronak and Eyre, 2016). While our estimates of oxygen fluxes are similar to results of *in-situ* studies on the Davies Reef lagoon (Table 3), the P/R of $2\text{--}2.4$ in our study is much higher than the $0.4\text{--}1.2$ found *in-situ* (Hansen et al., 1987, 1992). Thus, our dissolution estimates will likely underestimate the dissolution occurring in the lagoon sediments. However, benthic photosynthesis and respiration in reef sediments were shown to have a strong and linear control over dissolution (Cyronak et al., 2013b). We therefore estimated present day and future

TABLE 3 | Present and future *in-situ* dissolution rates on the Davis Reef lagoon were predicted using oxygen flux data from available literature and the linear relationship between dissolution and oxygen efflux from Figure 7.

Study	Oxygen efflux (mmol O ₂ m ⁻² d ⁻¹)	Estimated <i>in-situ</i> dissolution (mmol CaCO ₃ m ⁻² d ⁻¹)	
		Present day	1300 μ atm pCO ₂
Hansen et al., 1987	Night	−19.2 to −76.7	5.6 to 16.0
	Day	23.3 to 106.7	−17.0 to −2.0
	Daily	−10.0 to 15.0	−0.5 to 4.0
Hansen et al., 1992	Night	−7.0 to −38.2	3.4 to 9.0
	Day	−1.7 to 28.4	−2.9 to 2.5
	Daily	−0.9 to −7.1	2.3 to 3.5

dissolution rates using *in-situ* oxygen fluxes from Hansen et al. (1987, 1992) and the linear relation of dissolution vs. oxygen flux under control and high pCO₂ in our study (Figure 7). This results in present daily dissolution of −0.5 to 4.0 mmol CaCO₃ m⁻² d⁻¹ and future dissolution under high pCO₂ of 14.5 to 18.7 mmol CaCO₃ m⁻² d⁻¹ (Table 3). These dissolution rates can be regarded as maximum because they do not account for possibly lower porewater advection rates in the finer lagoon sands (median grain size 1.2–2.9 mm, Hansen et al., 1987). The increase in sediment dissolution due to porewater advection using the same stirring velocities as in our study (40 rpm) was shown to be 2.5 higher than under diffusive conditions (Cyronak et al., 2013a). Considering this, our estimates for future daily dissolution under diffusive conditions are 5.5 to 9.9 mmol CaCO₃ m⁻² d⁻¹, which can be considered minimum.

We estimated how such increases in dissolution rates relate to the accumulation rate of sediments into the lagoon and how it could affect the mineralogy. Maximum sediment accumulation rates on the Davies Reef lagoon during the last 4,000 years range between 1,800 and 3,600 g CaCO₃ m⁻² y⁻¹ or 1.3–2.5 mm y⁻¹ (Tudhope, 1983). Considering a sediment porosity of 0.5 and the density of calcite (2.71 g cm⁻³), the increase in dissolution under high pCO₂ could reduce sediment accumulation by 0.2–0.4 mm y⁻¹, thus by 6–31%. This could slow down reef accretion and make it harder for lagoons to keep up with future sea level rise.

Furthermore, the mineral composition of the lagoon sediments may drastically change due to the preferential dissolution of HMC. The accumulation of HMC in the lagoon can be calculated as 10% of the total sediment accumulation, thus 180–360 g CaCO₃ m⁻² y⁻¹ or 4.9–9.8 mmol CaCO₃ m⁻² d⁻¹. Since HMC are likely the predominantly dissolving minerals, even our minimum dissolution estimates under high pCO₂ could reduce the accumulation rates of HMC by at least 66%. This indicates that Davies Reef lagoon sediments could experience a fast decline in HMC, which has also been suggest for other coral reefs (Haese et al., 2014). This could lead toward a higher relative abundance of more stable minerals like aragonite (Andersson et al., 2007). Compared to HMC, more CO₂ is needed to reach undersaturating

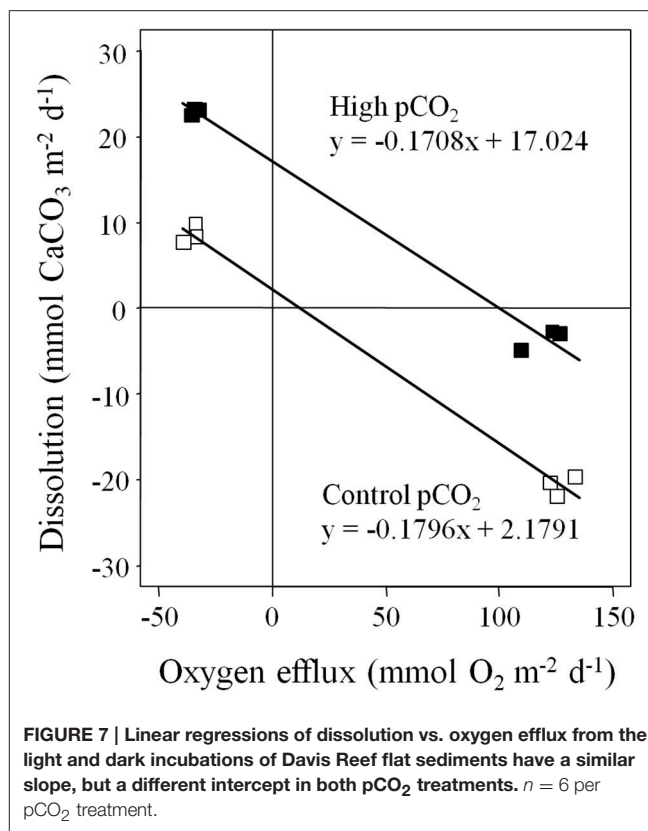


FIGURE 7 | Linear regressions of dissolution vs. oxygen efflux from the light and dark incubations of Davis Reef flat sediments have a similar slope, but a different intercept in both pCO₂ treatments. *n* = 6 per pCO₂ treatment.

conditions with respect to aragonite so that dissolution will then occur at a lower porewater pH that may affect sediment biota.

CONCLUSION

Our study contributes to the growing amount of evidence that coral reef sediment will dissolve faster in a high CO₂ world. The results of our study indicate that OA-induced sediment dissolution may have dramatic consequences for the carbonate budget of Davies Reef. It has the potential to reduce the sediment accumulation in the lagoon by up to 31%, which could result in the loss of invaluable reef space. Therefore, it is urgent to obtain present day estimates of dissolution rates and to perform *in-situ* acidification experiments, particularly on the deeper laying lagoon sediments. The data presented here suggest that high-magnesium calcites are the minerals predominantly dissolving and that the enhanced dissolution rates may drastically decrease their abundance in future sediments. While our relatively short experiments indicate that biotic processes will not be affected by OA, long-term dissolution could affect sediment properties that are crucial for efficient element cycling. Reef sediments are constantly eroding and dissolving to finer grains. A continuous supply of rubble from the reef framework is essential to maintain the coarse and highly permeable sediments. Increased sediment dissolution and reduced resupply of coarse sediments from reef organisms due to OA could reduce the grain size, and thus the permeability

of reef sediments. In mesocosm experiments using re-assembled coral reefs, a significant increase in the relative abundance of finer sediments has been demonstrated at high $p\text{CO}_2$ after 3 month (Dove et al., 2013), suggesting a decrease in permeability. Since high permeability of reef sediments is intimately linked to their function as biocatalytic filters of OM, this could reduce the efficient nutrient recycling on coral reefs and limit their productivity.

AUTHOR CONTRIBUTIONS

AF, SU, and DdB designed the study. AF, JdH, and AC collected the data. All authors were involved in data analysis and interpretation. AF wrote the manuscript with contribution from all other authors.

REFERENCES

- Albright, R., Langdon, C., and Anthony, K. R. N. (2013). Dynamics of seawater carbonate chemistry, production, and calcification of a coral reef flat, central Great Barrier Reef. *Biogeosciences* 10, 6747–6758. doi: 10.5194/bg-10-6747-2013
- Al-Najjar, M. A. A., de Beer, D., Kühl, M., and Polerecky, L. (2012). Light utilization efficiency in photosynthetic microbial mats. *Environ. Microbiol.* 14, 982–992. doi: 10.1111/j.1462-2920.2011.02676.x
- Andersson, A. J. (2015). A fundamental paradigm for coral reef carbonate sediment dissolution. *Front. Mar. Sci.* 2:52. doi: 10.3389/fmars.2015.00052
- Andersson, A. J., and Gledhill, D. (2013). Ocean acidification and coral reefs: effects on breakdown, dissolution, and net ecosystem calcification. *Annu. Rev. Mar. Sci.* 5, 321–348. doi: 10.1146/annurev-marine-121211-172241
- Andersson, A. J., Kuffner, I. B., Mackenzie, F. T., Jokiel, P. L., Rodgers, K. S., and Tan, A. (2009). Net Loss of CaCO_3 from a subtropical calcifying community due to seawater acidification: mesocosm-scale experimental evidence. *Biogeosciences* 6, 1811–1823. doi: 10.5194/bg-6-1811-2009
- Andersson, A., Bates, N., and Mackenzie, F. (2007). Dissolution of carbonate sediments under rising $p\text{CO}_2$ and ocean acidification: observations from devil's hole, Bermuda. *Aquat. Geochem.* 13, 237–264. doi: 10.1007/s10498-007-9018-8
- Anthony, K. R. N., Diaz-Pulido, G., Verlinden, N., Tilbrook, B., and Andersson, A. J. (2013). Benthic buffers and boosters of ocean acidification on coral reefs. *Biogeosciences* 10, 4897–4909. doi: 10.5194/bg-10-4897-2013
- Boudreau, B. P. (1997). *Diagenetic Models and their Implementation; Modelling Transport and Reactions in Aquatic Sediments*. New York, NY: Springer.
- Caldeira, K., and Wickett, M. E. (2003). Oceanography: anthropogenic carbon and ocean pH. *Nature* 425, 365–365. doi: 10.1038/425365a
- Chennu, A., Färber, P., Volkenborn, N., Al-Najjar, M. A. A., Janssen, F., de Beer, D., et al. (2013). Hyperspectral imaging of the microscale distribution and dynamics of microphytobenthos in intertidal sediments. *Limnol. Oceanogr. Methods* 11, 511–528. doi: 10.4319/lom.2013.11.511
- Chennu, A., Grinham, A., Polerecky, L., de Beer, D., and Al-Najjar, M. A. A. (2015). Rapid reactivation of cyanobacterial photosynthesis and migration upon rehydration of desiccated marine microbial mats. *Front. Microbiol.* 6:1472. doi: 10.3389/fmicb.2015.01472
- Chisholm, J. R. M., and Gattuso, J.-P. (1991). Validation of the alkalinity anomaly technique for investigating calcification of photosynthesis in coral reef communities. *Limnol. Oceanogr.* 36, 1232–1239. doi: 10.4319/lo.1991.36.6.1232
- Chung, F. H. (1974). Quantitative interpretation of X-ray diffraction patterns of mixtures. I. Matrix-flushing method for quantitative multicomponent analysis. *J. Appl. Crystallogr.* 7, 519–525.
- Comeau, S., Carpenter, R. C., Lantz, C. A., and Edmunds, P. J. (2015). Ocean acidification accelerates dissolution of experimental coral reef communities. *Biogeosciences* 12, 365–372. doi: 10.5194/bg-12-365-2015
- Comeau, S., Edmunds, P. J., Lantz, C. A., and Carpenter, R. C. (2014). Water flow modulates the response of coral reef communities to ocean acidification. *Sci. Rep.* 4:6681. doi: 10.1038/srep06681
- Cook, P. L. M., and Røy, H. (2006). Advective relief of CO_2 limitation in microphytobenthos in highly productive sandy sediments. *Limnol. Oceanogr.* 51, 1594–1601. doi: 10.4319/lo.2006.51.4.1594
- Cyronak, T., and Eyre, B. D. (2016). The synergistic effects of ocean acidification and organic metabolism on calcium carbonate (CaCO_3) dissolution in coral reef sediments. *Mar. Chem.* 183, 1–12. doi: 10.1016/j.marchem.2016.05.001
- Cyronak, T., Santos, I. R., and Eyre, B. D. (2013a). Permeable coral reef sediment dissolution driven by elevated $p\text{CO}_2$ and pore water advection. *Geophys. Res. Lett.* 40, 4876–4881. doi: 10.1002/grl.50948
- Cyronak, T., Santos, I. R., McMahon, A., and Eyre, B. D. (2013b). Carbon cycling hysteresis in permeable carbonate sands over a diel cycle: implications for ocean acidification. *Limnol. Oceanogr.* 58, 131–143. doi: 10.4319/lo.2013.58.1.0131
- Cyronak, T., Schulz, K. G., Santos, I. R., and Eyre, B. D. (2014). Enhanced acidification of global coral reefs driven by regional biogeochemical feedbacks. *Geophys. Res. Lett.* 41, 5538–5546. doi: 10.1002/2014GL060849
- de Beer, D., Schramm, A., Santegoeds, C. M., and Kühl, M. (1997). A nitrite microsensor for profiling environmental biofilms. *Appl. Environ. Microbiol.* 63, 973–977.
- de Beer, D., Wenzhöfer, F., Ferdelman, T. G., Boehme, S. E., Huettel, M., van Beusekom, J. E. E., et al. (2005). Transport and mineralization rates in North Sea sandy intertidal sediments, Sylt-Rømø Basin, Wadden Sea. *Limnol. Oceanogr.* 50, 113–127. doi: 10.4319/lo.2005.50.1.0113
- Dickson, A. G., Sabine, C. L., and Christian, J. R. (2007). *Guide to Best Practices for Ocean CO_2 Measurements*. Sidney: North Pacific Marine Science Organization.
- Dove, S. G., Kline, D. I., Pantos, O., Angly, F. E., Tyson, G. W., and Hoegh-Guldberg, O. (2013). Future reef decalcification under a business-as-usual CO_2 emission scenario. *Proc. Natl. Acad. Sci. U.S.A.* 110, 15342–15347. doi: 10.1073/pnas.1302701110
- Drupp, P. S., De Carlo, E. H., and Mackenzie, F. T. (2016). Porewater CO_2 –carbonic acid system chemistry in permeable carbonate reef sands. *Mar. Chem.* 185, 48–64. doi: 10.1016/j.marchem.2016.04.004
- Eyre, B. D., Andersson, A. J., and Cyronak, T. (2014). Benthic coral reef calcium carbonate dissolution in an acidifying ocean. *Nat. Clim. Change* 4, 969–976. doi: 10.1038/nclimate2380
- Haese, R. R., Smith, J., Weber, R., and Trafford, J. (2014). High-Magnesium calcite dissolution in tropical continental shelf sediments controlled by ocean acidification. *Environ. Sci. Technol.* 48, 8522–8528. doi: 10.1021/es501564q
- Hallock, P. (1997). “Reefs and reef limestones in Earth history,” in *Life and Death of Coral Reefs*, ed C. Birkeland (New York, NY: Chapman & Hall), 13–42.
- Hansen, J. A., Klumpp, D. W., Alongi, D. M., Dayton, P. K., and Riddle, M. J. (1992). Detrital pathways in a coral reef lagoon. *Mar. Biol.* 113, 363–372. doi: 10.1007/BF00349160

ACKNOWLEDGMENTS

We thank the MPI Microsensor group technicians for preparing the microsensors and M. Kebben for building the flumes. We are grateful to S. Noonan, K. Hohmann, and V. Hübner and the SeaSim technical staff for their continuous support during the experiments and C. Vogt for the XRD analyses. This study was funded by German Ministry for Research and Education (BMBF) project on the Biological Impacts of Ocean Acidification (BIOACID, grant 03F0666C) and a BMBF grant (01DR14002).

SUPPLEMENTARY MATERIAL

The Supplementary Material for this article can be found online at: <http://journal.frontiersin.org/article/10.3389/fmars.2017.00073/full#supplementary-material>

- Hansen, L. A., Alongi, D. M., Moriarty, D. J. W., and Pollard, P. C. (1987). The dynamics of benthic microbial communities at Davies Reef, central Great Barrier Reef. *Coral Reefs* 6, 63–70. doi: 10.1007/BF00301375
- Huettel, M., and Gust, G. (1992). Solute release mechanisms from confined sediment cores in stirred benthic chambers and flume flows. *Mar. Ecol. Prog. Ser. Oldendorf* 82, 187–197.
- Huettel, M., Berg, P., and Kostka, J. E. (2014). Benthic exchange and biogeochemical cycling in permeable sediments. *Annu. Rev. Mar. Sci.* 6, 23–51. doi: 10.1146/annurev-marine-051413-012706
- Huettel, M., Ziebis, W., and Forster, S. (1996). Flow-induced uptake of particulate matter in permeable sediments. *Limnol. Oceanogr.* 41, 309–322. doi: 10.4319/lo.1996.41.2.0309
- Janssen, F., Huettel, M., and Witte, U. (2005). Pore-water advection and solute fluxes in permeable marine sediments (II): benthic respiration at three sandy sites with different permeabilities (German Bight, North Sea). *Limnol. Oceanogr.* 50, 779–792. doi: 10.4319/lo.2005.50.3.0779
- Jørgensen, B. B. (1978). A comparison of methods for the quantification of bacterial sulfate reduction in coastal marine sediments: I. Measurement with radiotracer techniques. *Geomicrobiol. J.* 1, 11–27.
- Kallmeyer, J., Ferdelman, T. G., Weber, A., Fossing, H., and Jørgensen, B. B. (2004). A cold chromium distillation procedure for radiolabeled sulfide applied to sulfate reduction measurements. *Limnol. Oceanogr. Methods* 2, 171–180. doi: 10.4319/lom.2004.2.171
- Khatiwal, S., Tanhua, T., Mikaloff Fletcher, S., Gerber, M., Doney, S. C., Graven, H. D., et al. (2013). Global ocean storage of anthropogenic carbon. *Biogeosciences* 10, 2169–2191. doi: 10.5194/bg-10-2169-2013
- Klump, D. W., and McKinnon, A. D. (1989). Temporal and spatial patterns in primary production of a coral-reef epilithic algal community. *J. Exp. Mar. Biol. Ecol.* 131, 1–22. doi: 10.1016/0022-0981(89)90008-7
- Klute, A., and Dirksen, C. (1986). “Hydraulic conductivity and diffusivity: laboratory methods,” in *Methods of Soil Analysis. Part 1. Physical and Mineralogical Methods*, ed A. Klute (Madison, WI: American Society of Agronomy), 687–734.
- Langdon, C., Broecker, W. S., Hammond, D. E., Glenn, E., Fitzsimmons, K., Nelson, S. G., et al. (2003). Effect of elevated CO₂ on the community metabolism of an experimental coral reef. *Glob. Biogeochem. Cycles* 17:1011. doi: 10.1029/2002gb001941
- Lavigne, H., Epitalon, J.-M., and Gattuso, J.-P. (2011). *Seacarb: Seawater Carbonate Chemistry with R. R Package Version 3.0*. Available online at: <http://CRAN.R-project.org/package=seacarb>
- Leclercq, N., Gattuso, J.-P., and Jaubert, J. (2002). Primary production, respiration, and calcification of a coral reef mesocosm under increased CO₂ partial pressure. *Limnol. Oceanogr.* 47, 558–564. doi: 10.4319/lo.2002.47.2.0558
- Morse, J. W., Andersson, A. J., and Mackenzie, F. T. (2006). Initial responses of carbonate-rich shelf sediments to rising atmospheric pCO₂ and “ocean acidification”: role of high Mg-calcites. *Spec. Issue Dedic. Robert Bern.* 70, 5814–5830. doi: 10.1016/j.gca.2006.08.017
- Moss, R. H., Edmonds, J. A., Hibbard, K. A., Manning, M. R., Rose, S. K., van Vuuren, D. P., et al. (2010). The next generation of scenarios for climate change research and assessment. *Nature* 463, 747–756. doi: 10.1038/nature08823
- Orr, J. C., Fabry, V. J., Aumont, O., Bopp, L., Doney, S. C., Feely, R. A., et al. (2005). Anthropogenic ocean acidification over the twenty-first century and its impact on calcifying organisms. *Nature* 437, 681–686. doi: 10.1038/nature04095
- Ow, Y. X. (2016). *Interactive Effects of Ocean Acidification and Declining Water Quality on Tropical Seagrass Physiology*. Ph.D. thesis, James Cook University, Townsville.
- Pickard, G. L. (1986). Effects of wind and tide on upper-layer currents at Davies Reef, Great Barrier Reef, during MECOR (July–August 1984). *Aust. J. Mar. Freshw. Res.* 37, 545–565. doi: 10.1071/MF9860545
- Plummer, L. N., and Mackenzie, F. T. (1974). Predicting mineral solubility from rate data; application to the dissolution of magnesian calcites. *Am. J. Sci.* 274, 61–83. doi: 10.2475/ajs.274.1.61
- Polerecky, L., Bachar, A., Schoon, R., Grinstein, M., Jørgensen, B. B., De Beer, D., et al. (2007). Contribution of Chloroflexus respiration to oxygen cycling in a hypersaline microbial mat from Lake Chiprana, Spain. *Environ. Microbiol.* 9, 2007–2024. doi: 10.1111/j.1462-2920.2007.01317.x
- Polerecky, L., Bissett, A., Al-Najjar, M., Faerber, P., Osmers, H., Suci, P. A., et al. (2009). Modular spectral imaging system for discrimination of pigments in cells and microbial communities. *Appl. Environ. Microbiol.* 75, 758–771. doi: 10.1128/AEM.00819-08
- Poppe, L. J., Eliason, A. H., and Hastings, M. E. (2004). A visual basic program to generate sediment grain-size statistics and to extrapolate particle distributions. *Comput. Geosci.* 30, 791–795. doi: 10.1016/j.cageo.2004.05.005
- R Core Team (2015). *R: A Language and Environment for Statistical Computing*. R Found. Stat. Comput. Available online at: <https://www.R-Project.org>
- Rao, A. M. F., Polerecky, L., Ionescu, D., Meysman, F. J. R., and de Beer, D. (2012). The influence of pore-water advection, benthic photosynthesis, and respiration on calcium carbonate dynamics in reef sands. *Limnol. Oceanogr.* 57, 809–825. doi: 10.4319/lo.2012.57.3.0809
- Rasheed, M., Badran, M. I., Richter, C., and Huettel, M. (2002). Effect of reef framework and bottom sediment on nutrient enrichment in a coral reef of the Gulf of Aqaba, Red Sea. *Mar. Ecol. Prog. Ser.* 239, 277–285. doi: 10.3354/meps239277
- Reinfelder, J. R. (2011). Carbon concentrating mechanisms in eukaryotic marine phytoplankton. *Annu. Rev. Mar. Sci.* 3, 291–315. doi: 10.1146/annurev-marine-120709-142720
- Revsbech, N. P. (1989). An oxygen microsensor with a guard cathode. *Limnol. Oceanogr.* 34, 474–478.
- Reyes-Nivia, C., Diaz-Pulido, G., Kline, D., Guldborg, O.-H., and Dove, S. (2013). Ocean acidification and warming scenarios increase microbioerosion of coral skeletons. *Glob. Change Biol.* 19, 1919–1929. doi: 10.1111/gcb.12158
- Røy, H., Weber, H. S., Tarpgaard, I. H., Ferdelman, T. G., and Jørgensen, B. B. (2014). Determination of dissimilatory sulfate reduction rates in marine sediment via radioactive ³⁵S tracer. *Limnol. Oceanogr. Methods* 12, 196–211. doi: 10.4319/lom.2014.12.196
- Ryle, V. D., Mueller, H. R., and Gentien, P. (1981). *Automated Analysis of Nutrients in Tropical Seawaters*. Australian Institute of Marine Science.
- Schoon, R., Bissett, A., and de Beer, D. (2010). Resilience of pore-water chemistry and calcification in photosynthetic zones of calcifying sediments. *Limnol. Oceanogr.* 55, 377–385. doi: 10.4319/lo.2010.55.1.0377
- Sultana, R., Casareto, B. E., Sohrin, R., Suzuki, T., Alam, M. S., Fujimura, H., et al. (2016). Response of subtropical coastal sediment systems of okinawa, japan, to experimental warming and high pCO₂. *Front. Mar. Sci.* 3:100. doi: 10.3389/fmars.2016.00100
- Trnovsky, D., Stoltenberg, L., Cyronak, T., and Eyre, B. D. (2016). Antagonistic effects of ocean acidification and rising sea surface temperature on the dissolution of coral reef carbonate sediments. *Front. Mar. Sci.* 3:211. doi: 10.3389/fmars.2016.00211
- Tudhope, A. W. (1983). *Processes of Lagoonal Sedimentation and Patch Reef Development, Davies Reef, Great Barrier Reef of Australia*. Ph.D. thesis, University of Edinburgh.
- Uthicke, S., and Klump, D. W. (1998). Microphytobenthos community production at a near-shore coral reef: seasonal variation and response to ammonium recycled by holothurians. *Mar. Ecol. Prog. Ser.* 169, 1–11. doi: 10.3354/meps169001
- Uthicke, S., Furnas, M., and Lønborg, C. (2014). Coral Reefs on the edge? carbon chemistry on Inshore Reefs of the Great Barrier Reef. *PLOS ONE* 9:e109092. doi: 10.1371/journal.pone.0109092
- van Hoytema, N., Bednarz, V. N., Cardini, U., Naumann, M. S., Al-Horani, F. A., and Wild, C. (2016). The influence of seasonality on benthic primary production in a Red Sea coral reef. *Mar. Biol.* 163:52. doi: 10.1007/s00227-015-2787-5
- Vogel, N., Cantin, N. E., Strahl, J., Kaniewska, P., Bay, L., Wild, C., et al. (2016). Interactive effects of ocean acidification and warming on coral reef associated epilithic algal communities under past, present-day and future ocean conditions. *Coral Reefs* 35, 715–728. doi: 10.1007/s00338-015-1392-x
- Werner, U., Bird, P., Wild, C., Ferdelman, T., Polerecky, L., Eickert, G., et al. (2006). Spatial patterns of aerobic and anaerobic mineralization rates and oxygen

- penetration dynamics in coral reef sediments. *Mar. Ecol. Prog. Ser.* 309, 93–105. doi: 10.3354/meps309093
- Werner, U., Blazejak, A., Bird, P., Eickert, G., Schoon, R., Abed, R. M. M., et al. (2008). Microbial photosynthesis in coral reef sediments (Heron Reef, Australia). *Estuar. Coast. Shelf Sci.* 76, 876–888. doi: 10.1016/j.ecss.2007.08.015
- Wild, C., Rasheed, M., Werner, U., Franke, U., Johnstone, R., and Huettel, M. (2004). Degradation and mineralization of coral mucus in reef environments. *Mar. Ecol. Prog. Ser.* 267, 159–171. doi: 10.3354/meps267159
- Wisshak, M., Schönberg, C. H. L., Form, A., and Friwald, A. (2012). Ocean acidification accelerates reef bioerosion. *PLoS ONE* 7:e45124. doi: 10.1371/journal.pone.0045124
- Wright, S., Jeffrey, S., Mantoura, R., Llewellyn, C., Bjornland, T., Repera, D., et al. (1991). Improved HPLC method for the analysis of chlorophylls and carotenoids from marine phytoplankton. *Mar. Ecol. Prog. Ser.* 77, 183–196.
- Yamamoto, S., Kayanne, H., Tokoro, T., Kuwae, T., and Watanabe, A. (2015). Total alkalinity flux in coral reefs estimated from eddy covariance and sediment pore-water profiles. *Limnol. Oceanogr.* 60, 229–241. doi: 10.1002/lno.10018
- Zeebe, R. E., and Wolf-Gladrow, D. (2001). *CO₂ in Seawater: Equilibrium, Kinetics, Isotopes*. Amsterdam: Elsevier Oceanogr. Ser. 65 Amst.
- Conflict of Interest Statement:** The authors declare that the research was conducted in the absence of any commercial or financial relationships that could be construed as a potential conflict of interest.

Copyright © 2017 Fink, den Haan, Chennu, Uthicke and de Beer. This is an open-access article distributed under the terms of the Creative Commons Attribution License (CC BY). The use, distribution or reproduction in other forums is permitted, provided the original author(s) or licensor are credited and that the original publication in this journal is cited, in accordance with accepted academic practice. No use, distribution or reproduction is permitted which does not comply with these terms.